Intensity modulated operating mode of the rotating gamma system

Bishwambhar Sengupta
Department of Physics and Astronomy, Clemson University, Clemson, SC 29634, USA

Laszlo Gulyas
Rotating Gamma Institute, Debrecen H-4032, Hungary

Donald Medlin
Department of Physics and Astronomy, Clemson University, Clemson, SC 29634, USA

Tibor Koroknai, David Takacs, Gyorgy Filep, Peter Panko, and Bence Godo
Medikai Innovacio Kft, Debrecen H-4026, Hungary

Tamas Hollo
Rotating Gamma Institute, Debrecen H-4032, Hungary

Xiao Ran Zheng
Department of Physics and Astronomy, Clemson University, Clemson, SC 29634, USA

Imre Fedorcsak, Jozsef Dobai, and Laszlo Bognar
Department of Neurosurgery, University of Debrecen, Debrecen H-4032, Hungary

Endre Takacs[a)]
Department of Physics and Astronomy, Clemson University, Clemson, SC 29634, USA

(Received 5 January 2018; revised 19 February 2018; accepted for publication 6 March 2018; published 17 April 2018)

Purpose: The purpose of this work was to explore two novel operation modalities of the rotating gamma systems (RGS) that could expand its clinical application to lesions in close proximity to critical organs at risk (OAR).
Methods: The approach taken in this study consists of two components. First, a Geant4-based Monte Carlo (MC) simulation toolkit is used to model the dosimetric properties of the RGS Vertex 360™ for the normal, intensity modulated radiosurgery (IMRS), and speed modulated radiosurgery (SMRS) operation modalities. Second, the RGS Vertex 360™ at the Rotating Gamma Institute in Debrecen, Hungary is used to collect experimental data for the normal and IMRS operation modes. An ion chamber is used to record measurements of the absolute dose. The dose profiles are measured using Gafchromic EBT3 films positioned within a spherical water equivalent phantom.
Results: A strong dosimetric agreement between the measured and simulated dose profiles and penumbra was found for both the normal and IMRS operation modes for all collimator sizes (4, 8, 14, and 18 mm diameter). The simulated falloff and maximum dose regions agree better with the experimental results for the 4 and 8 mm diameter collimators. Although the falloff regions align well in the 14 and 18 mm collimators, the maximum dose regions have a larger difference. For the IMRS operation mode, the simulated and experimental dose distributions are ellipsoidal, where the short axis aligns with the blocked angles. Similarly, the simulated dose distributions for the SMRS operation mode also adopt an ellipsoidal shape, where the short axis aligns with the angles where the orbital speed is highest. For both modalities, the dose distribution is highly constrained with a sharper penumbra along the short axes.
Conclusions: Dose modulation of the RGS can be achieved with the IMRS and SMRS modes. By providing a highly constrained dose distribution with a sharp penumbra, both modes could be clinically applicable for the treatment of lesions in close proximity to critical OARs. © *2018 American Association of Physicists in Medicine* [https://doi.org/10.1002/mp.12887]

Key words: Geant4-based Monte Carlo simulation, intensity modulation, radiosurgery, rotating gamma system, speed modulation

1. INTRODUCTION

Stereotactic radiosurgery (SRS) is being used for the treatment of benign and malignant tumors, vascular malformations, and functional disorders. It employs 3D target localization to guide several finely collimated pencil radiation beams to deliver a single, precisely localized, high dose of targeted radiation. RGS Vertex 360™ rotating gamma system (RGS) apply 30 cobalt-60 gamma radiation sources that rotate around the long axis of the patient's body.[1] The

collimators are part of two concentric hemispheres that rotate in synchrony around the patient's body with a preset constant angular velocity, producing a close to spherical dose distribution at the isocenter of the device. The narrow penumbra of the machine is due to the sharp dose falloff resulting in the various entrance angles the rotation produces. The effect is comparable to the dose distribution delivered by the Gamma Knife® type devices that employ a large number of static sources.[2] Intracranial radio surgical treatments performed with various types of devices have been well documented in the literature,[2–5] but papers describing the dosimetric capabilities of the RGS-type machines are sparse.[1,6–8]

Highly accurate dose delivery representative of Gamma Knifes® and RGS devices is especially important for the treatment of cases near critical structures of the brain. Trigeminal neuralgia (TN), for example — a form of chronic, debilitating neuropathic pain — is one of the cases, where the use of these machines is desirable, but the application depends on the particular case due to the closeness of the brainstem. TN is caused by pressure on the trigeminal nerve from nearby blood vessels or tumors, by the damage of the trigeminal myelin sheath, or by nearby arteriovenous malformations.[9] If medications fail to reduce pain or lead to adverse side effects, then surgical techniques, including SRS, maybe applied.[10,11] The effective treatment of TN with SRS depends primarily on the precise delivery of a high dose of radiation, in the order of 75 to 90 Gy, to the trigeminus nerve, however, SRS can only be used for the treatment of TN when the dose spillage to the brain stem can be minimized.[12] In order to, create a sharp dose falloff (high selectivity), while depositing high dosage of radiation (high conformity) to treat TN and similar disorders near critical structures of the brain intensity modulated operation of the RGS has been proposed[13] (Intensity Modulated Radiation Surgery, IMRS).

IMRS can deliver both high selectivity and high conformity by providing a sculpted dose intensity distribution, as opposed to the spherical dose distribution. The shaping of the dose distribution can be achieved when the sources and collimators rotate asynchronously in certain angular positions to block the radiation beams at those angles. Although IMRS in connection with gamma knife[14] and various RGS devices has been proposed in the literature[13] as an intrinsic capability stemming from the rotation of the sources, this technique has not been studied dosimetrically or demonstrated in practice to date.

In this paper, we describe the efforts of the Medical Physics research group of the Department of Physics and Astronomy at Clemson University (CU) to model the IMRS operation of an RGS system in service at the Rotating Gamma Institute (RGI) in Debrecen, Hungary. In the following, we present our modeling and experimental procedures and demonstrate that adequately modified dose distributions can be produced by the IMRS operation of the RGS by blocking the radiation from certain directions. This method could potentially expand the applicability of the RGS to previously untreatable cases of trigeminal neuralgia and other similarly high-risk conditions. Results of the calculations have been compared with dosimetric measurements at RGI.

As an extension to the blocked angle IMRS mode, this paper also describes our studies of another operational modality of the RGS that could have a critical clinical impact. This modality is called Speed Modulated Radiation Surgery (SMRS) and works by modulating the rotational speed of the cobalt-60 sources with a predetermined mathematical function of the rotation angle. SMRS can produce dose distributions that are geometrically different from the spherical distribution created while operating at a constant angular velocity. The proposed SMRS modality of the RGS may increase the envelope, precision, and control of the dose distribution without compromising the penumbra achievable with IMRS with a greatly improved treatment time. This would enable the use of the RGS for cases of TN and other treatment indications in close proximity to critical tissues that the RGS could not treat otherwise.

2. MATERIALS AND METHODS

2.A. Rotating gamma system in Debrecen, Hungary

The rotating gamma system at the Rotating Gamma Institute in Hungary (RGS Vertex 360™ by American Radiosurgery Inc., San Diego, CA, USA) has been in operation since 2007. Its geometry and design are similar to the instrument reported by Goetsch et al.[1] It consists of a hemispherical shell made of cast iron, which contains the source body that houses the sources and performs the primary collimation. The sources are placed in one sector with latitude angles ranging from 14.3° to 52° sector angle 72° [Fig. 1(a)].

A second concentric hemispherical shell contains the secondary collimators to produce approximately spherical dose distributions with 50% width having diameters 4 mm, 8 mm, 14 mm, and 18 mm [Fig. 1(b)]. There is a fifth set of collimators in this shell, which contain tungsten plugs to block the radiation when aligned with the sources in the so-called "0" or home position. The sources and collimators are placed such that, when aligned, the intersection point of all the gamma beams is 3 cm outside from the center of the hemisphere along the axis of rotation of the shells to extend the reach of the instrument toward the upper neck region. The system incorporates a patient positioning system capable of movement along three directions.

2.B. Dosimetry of the RGS and analysis of experimental data

Absolute dose measurements were performed by a 3D pinpoint ion chamber together with an electrometer from PTW GmbH. The chamber has an active volume of 0.016 cm^3 filled with argon gas. The electrometer and the ion chamber

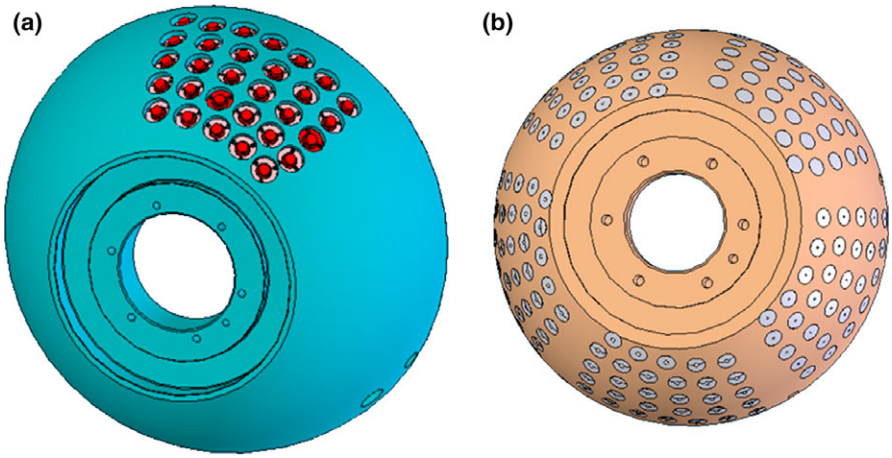

FIG. 1. (a) The primary collimator body and (b) the secondary collimator body. [Color figure can be viewed at wileyonlinelibrary.com]

were both calibrated by the manufacturer to an accuracy of 1.1%. The chamber was placed inside a 16 cm water equivalent phantom and was radiated for 1 min with the 18 mm collimator to infer the absolute dose rate achievable with this collimation. Ten independent dose rate measurements were taken with an average value of 3.2 Gy/min. This dose rate was entered into the Treatment Planning Software (TPS) and was used throughout these experiments.

In order to measure the spatial dose distribution, Gafchromic EBT3 (External Beam Radiotherapy, Ashland) films were used. The films were scanned using an Epson V850 Pro Scanner at 72 dpi resolution, as was recommended by the manufacturer. The films were placed at the center of the spherical 16 cm diameter water equivalent phantom and were positioned to the isocenter of the machine during the irradiations. The rotational speed of the RGS was between 1 and 4 rpms, and the films received a total dose between 6 and 8 Gy. The films were processed with the film evaluation software (FilmQAPro) provided by the vendor to generate the dosimetric distribution data.

Calibration of the films was performed by comparing the measured dosimetric properties obtained from films that were irradiated with predefined doses, which were validated with ionization chamber measurements. This was performed sequentially for six strips of film. For each measurement, scans of zero intensity and high-intensity reference films were also taken simultaneously to account for the measurement uncertainties. Data from the red channel of the scanned RGB color image were used for comparisons of the dosimetric profiles with those determined by simulation.

2.C. RGS operation in IMRS mode

The rotational motion of both the source body and the secondary collimator is controlled by a 5-axis microcontroller within the RGS's electronic control system. During normal operation, the microcontroller initially rotates both the primary and the secondary collimator bodies to their home position synchronously. The microcontroller selects the appropriate collimator by changing the angular velocity of the secondary collimator body until the desired collimator is aligned with the sources, after which both bodies are moved synchronously to maintain this alignment. These collimators

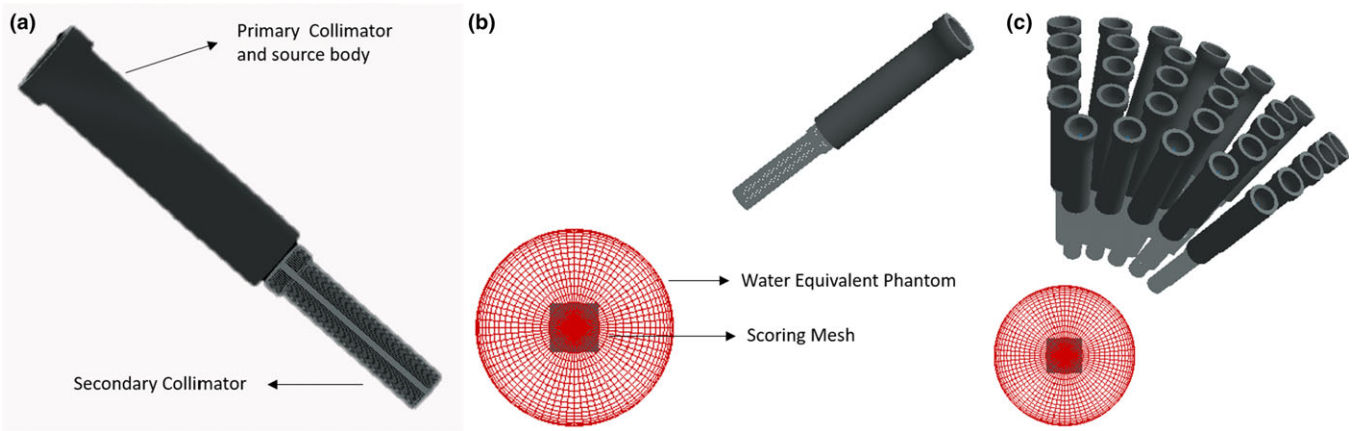

FIG. 2. Illustration of (a) the source along with the secondary collimator, (b) position of one source with respect to the water equivalent phantom, and (c) position of all sources with respect to the phantom used in the simulation with detector at the center. [Color figure can be viewed at wileyonlinelibrary.com]

are rotated around the axis of the hemispheres at a constant angular velocity, which produces a close to spherical dose distribution.

In contrast, nonspherical dose distributions can be achieved with the RGS while operating in the IMRS mode, where the radiation is blocked at preselected angular positions during the treatment. Blocking is achieved by misaligning the primary and secondary collimator bodies as they rotate through the angular regions where incoming radiation is not desired. In collaboration with the manufacturer, the microcontroller code was modified to allow for IMRS with the RGS. Modifications to the treatment planning software were also made to accommodate the IMRS mode; e.g., halting the timer whenever the radiation is blocked during the treatment to account for the proper dose delivery time.

Measurements to study the spatial dosimetric distribution of the IMRS mode were the same as described in the previous section with the angular regions between 61° and 180° and 241° and 360° blocked.

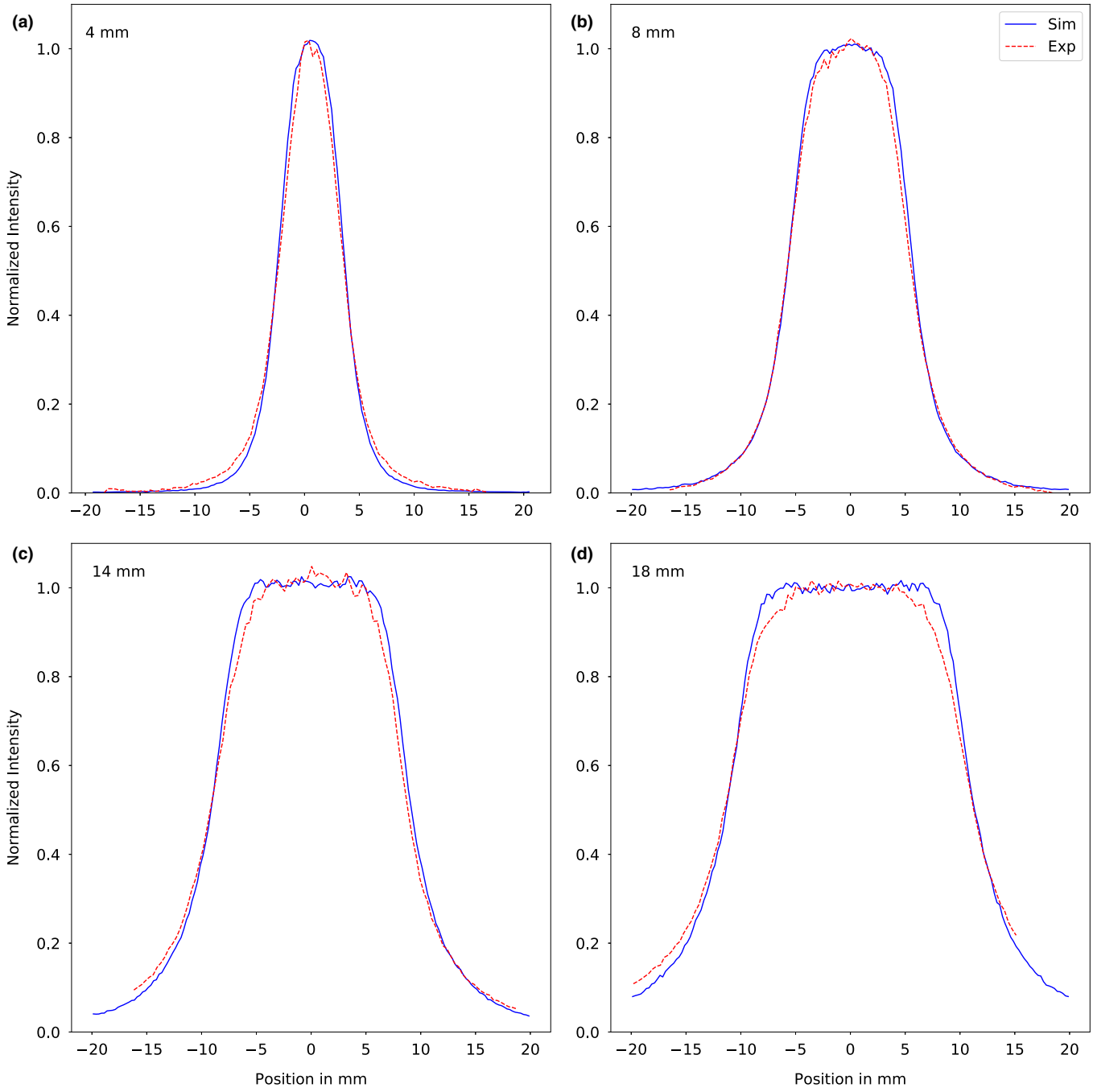

FIG. 3. Profile comparison of the simulation and the experimental data of the *X*-axis of the XY plane for the four collimator sizes of the RGS; (a) 4 mm, (b) 8 mm, (c) 14 mm, and (d) 18 mm. [Color figure can be viewed at wileyonlinelibrary.com]

2.D. Monte Carlo simulation

The simulations for this study were performed using the Geant4 simulation package, which is a Monte Carlo simulation toolkit developed and maintained by the Geant4 collaboration.[15–18] Its predecessor was developed to run simulations of high energy physics at CERN but it has also found applications in various other fields including medical physics. To reduce the simulation time, the parallel computing capabilities of the Geant4 package were taken advantage of by running it on the Palmetto Cluster of Clemson University.

Version 10.03.p01 of the Geant4 toolkit was used to for the dose calculations of the RGS. Similar to the Gamma Knife sample code provided with the toolkit, we introduced a general particle source (GPS), which defines the specifications of the spectral, spatial, and angular distribution of the primary source particles. The RGS geometry was modeled with the built-in Geant4 geometrical elements, which allows the user to specify the material, spatial position as well as the logical relations among the components. A combination of the G4Polycone class and Boolean solids worked best to precisely model the RGS geometry according to the manufacturer's design drawings.

The 30 Co-60 sources in the RGS were modeled with source cylinders of the exact same dimensions and were positioned within the source cavity inside the primary collimator made of cast iron. The secondary collimator body was positioned within the primary collimator body and the collimators were aligned with the center of the water equivalent phantom. The water equivalent phantom was placed at the center of the geometry world.

Generation of the primary particles (gamma photons) occurs inside the source capsules. The GPS allows the user to specify a volume of any dimension, location, and orientation, inside which the particles will be created. To accurately model the gamma photon generation, two GPS objects with mono-energetic distributions of energies 1.33 and 1.17 MeV[19] were generated. The primary particles were generated with an isotropic angular distribution, however, a limit of 3 degrees was placed on the θ distribution to increase the simulation's efficiency,[20] with the assumption that gamma photons leaving the source capsule in the real system outside this cone do not contribute much to the overall dose distribution at the isocenter.

Geant4 offers a command based scoring mechanism through the G4ScoringManager class. It utilizes parallel navigation in a parallel world volume, so the user can define a three-dimensional mesh and scoring independently from the physical geometry. To accurately model the Gafchromic films used to measure the experimental dose distributions, we created a scoring mesh with equivalent dimensions (40 mm × 40 mm × 1 mm) that was split into 160 × 160 × 1 cubic bins. The detectors were set to record the dose deposited in units of Gy along with the total energy in MeV. Exploiting the symmetry of device, the scoring mesh was rotated along its z-axis to model the rotation of the treatment head, which resulted in a considerable simplification of the geometry code.[20]

For tracking the photons and particles, the Reference Physics List simulation engine: QGSP\BIC 4.0 EMoption= 3 recommended for medical applications[21] was used. The primary particle loses energy by producing secondary electrons or gamma photons. In Geant4, the threshold for secondary particle production is defined in distance rather than energy. If the primary particle has insufficient energy to generate secondary particles that travel at least 1 mm into the surrounding material, then no secondary particles are produced and the primary particle loses energy due to continuous energy loss. Thus, the stopping location of the

TABLE I. Comparison of the profile widths between experiment and simulation. All penumbra values are calculated as (90% width – 50% width)/2 and are shown in mm.

	Experiment (mm)			Simulation (mm)		
Collimator size	90%	50%	Penumbra	90%	50%	Penumbra
4	2.82	6.02	1.6	3.12	6.21	1.55
8	6.54	11.11	2.13	7.31	11.53	2.11
14	12.26	17.61	2.68	13.59	18.62	2.14
18	15.83	22.16	3.17	17.26	22.83	2.79

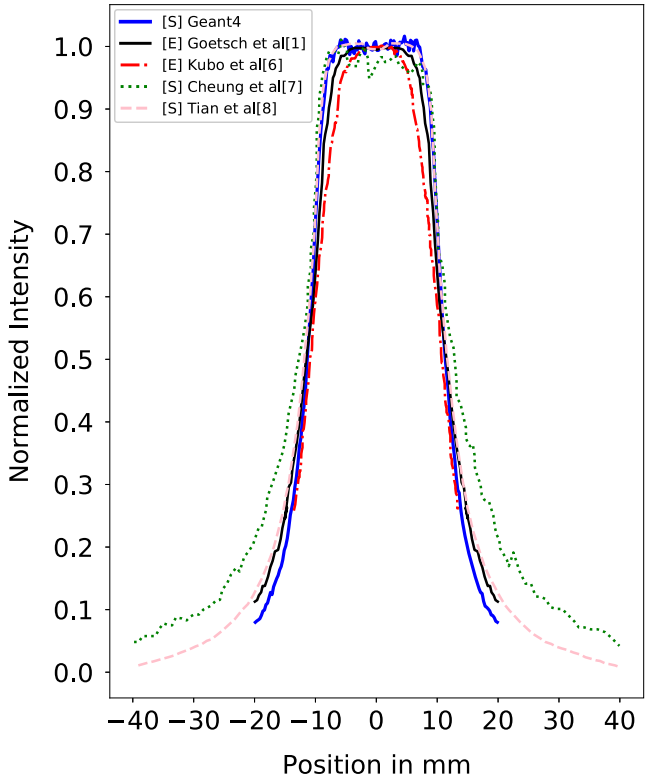

FIG. 4. Comparison of X profiles of different RGS devices and their simulation. [S] represents simulation data and [E] represents experimental data. [Color figure can be viewed at wileyonlinelibrary.com]

primary particle is accurate. This allows for the use of distance as the only parameter for the production threshold since the percentage depth dose (PDD) depends on the material. This distance was set to 1 mm after a series of experiments with different values to optimize our simulation time and provide accurate results given the statistical nature of the absorption.

Regarding the runtime, it takes approximately 3 h for an Intel®Xeon®CPUE5345 processor to run simulations with the generation of 10^7 primary particles. During the dosimetric modeling of the RGS, we generally used 3.6×10^{10} primary particles to create sufficient statistics for evaluating the dose distributions.

In order to validate the GEANT4 simulation package, we have compared the results with experimental data from the RGS during the normal operation mode, where the sources maintain a constant angular velocity and produce a close to spherical dose distribution. After validation, the simulation package was used to predict the dosimetric properties of the RGS for the IMRS operation mode and compared with experimental data. Lastly, the simulation platform was used to model the dose distribution of the RGS during the proposed SMRS modality by using harmonic angle-to-speed functions. A part of the geometry created by our code is shown in Fig. 2.

3. RESULTS

3.A. Normal operation mode of the RGS

In the normal operation mode, the RGS produces a near spherical dose distribution at the isocenter. To validate the accuracy of our simulation platform and RGS model, the simulated dose profiles and penumbrae in a water phantom were compared with those obtained experimentally for identical conditions. The dosimetric film was located in the XY plane, perpendicular to the longitudinal axis of the patient (Z), with the *Y*-axis in the vertical direction.

Comparisons of the measured and simulated results for the four collimators are shown in Fig. 3. Similar shapes near the top of the distribution have been observed in previous simulations.[7,8] The penumbra width was calculated by taking half the difference between the 90% and 50% widths, similar to Kubo et al.[6] Table I shows the tabulated values of the 50% and 90% widths for the experimental and simulated data.

As with the dose profiles, the agreement between the experimental and simulated penumbra widths are better for the 4 and 8 mm collimators compared to the 14 and 18 mm collimators. At the 50% width, the simulation and the experiment profiles closely match each other. Near the maximum dose regions, the experimental profile falls off faster causing

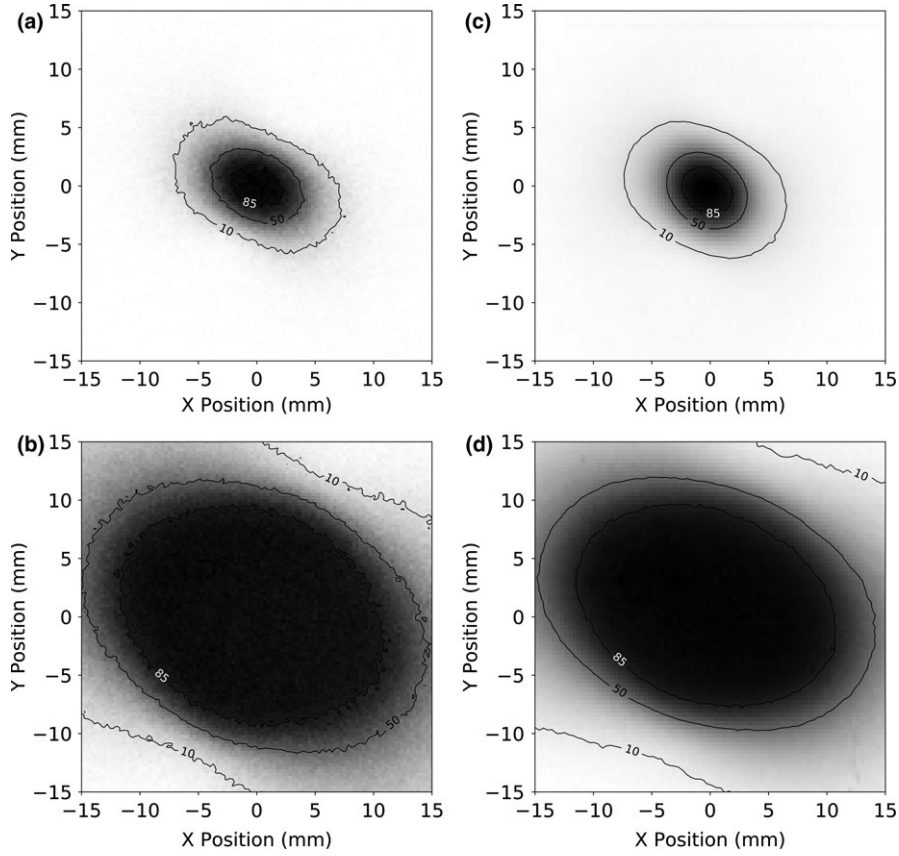

FIG. 5. Intensity modulated radio surgery (IMRS) mode of RGS comparing the dose delivered by the 4 mm and the 18 mm collimator between the Simulation (a), (b) and Experiment (c), (d).

the experimental penumbra to be slightly larger than that obtained from the simulations, with the maximum difference of 0.76 mm for the 18 mm collimator and minimum of 0.05 mm for the 8 mm collimator.

In order to compare different RGS devices and models described in the literature, we have included their 18 mm collimator X profiles in Fig. 4.

The experimental and simulated results from these studies show good agreement, which indicates that different RGS-type machines produce similar dose distributions with slight changes to the profile, as shown in Fig. 4. The UC Davis machine's design was changed on the site during installation which might have led to a narrower falloff as described in the work by Kubo et al.[6]

3.B. IMRS operation mode of the RGS

To study the dose distributions for the IMRS operation mode of the RGS, the radiation was blocked for orbital angles from 61° to 180° and 241° to 360° for both the simulated and experimental tests. The resulting dose distributions were no longer spherically symmetric since the incoming radiation is blocked from two opposite directions. The dose distributions adopted an ellipsoid shape as the irradiated region is shorter along the direction of the blocked angles than those for the unblocked angles. This is evident from the elliptic dose distribution displayed on the Gafchromic films shown in Figs. 5(a) and 5(b) for the 4 and 18 mm diameter collimators, respectively.

A comparison of the dose profiles along those two directions is shown in Fig. 6. The 90% and 50% widths along the blocked directions are shorter than those along the unblocked directions. Furthermore, the penumbra is considerably sharper along the short axis of the dose distribution than that of the long axis and those measured during the normal operation mode.

3.C. Speed modulation mode of the RGS

Even though the IMRS operation mode of the RGS offers a sharp falloff as demonstrated in the previous section, one apparent disadvantage is that the sources are off for a considerable fraction of the time. The additional time needed to deliver the desired dose will depend on the ratio of the total angles blocked to the total angles traversed. In this study, the use of the IMRS modality results in a threefold increase in delivery time, which is impractical for the treatment of conditions that require a high dose. To circumvent the increased treatment time while maintaining the benefits of the IMRS mode, we simulated a novel operation mode of the RGS, called the speed modulated radiosurgery (SMRS) mode. Instead of blocking the radiation at certain angles, in the SMRS mode, the orbital speed of the RGS is modulated as a function of its angle around the patient. Figure 7 shows the

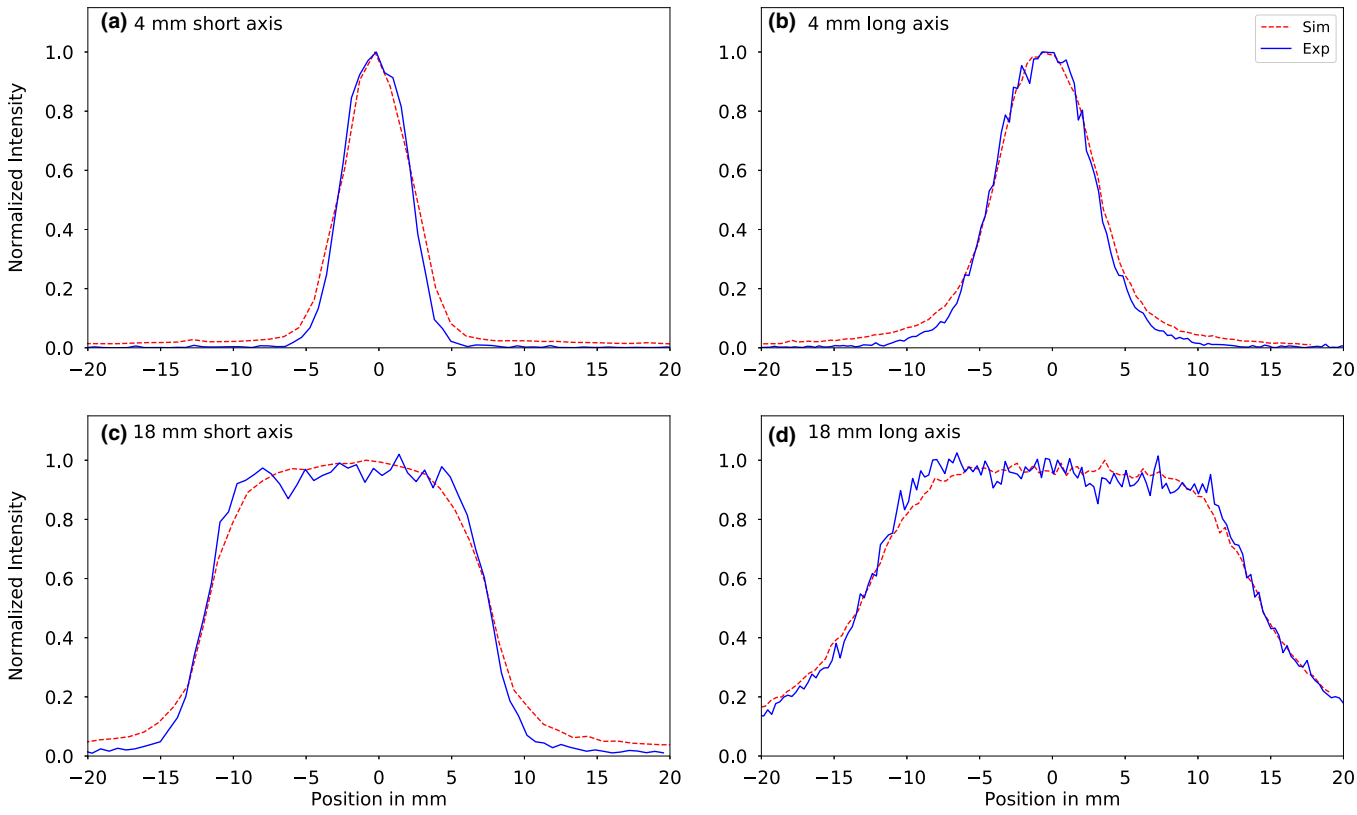

FIG. 6. Profile comparison along the short and long axis for the intensity modulated operation in 4 mm (a), (b) and 18 mm (c), (d) configuration. [Color figure can be viewed at wileyonlinelibrary.com]

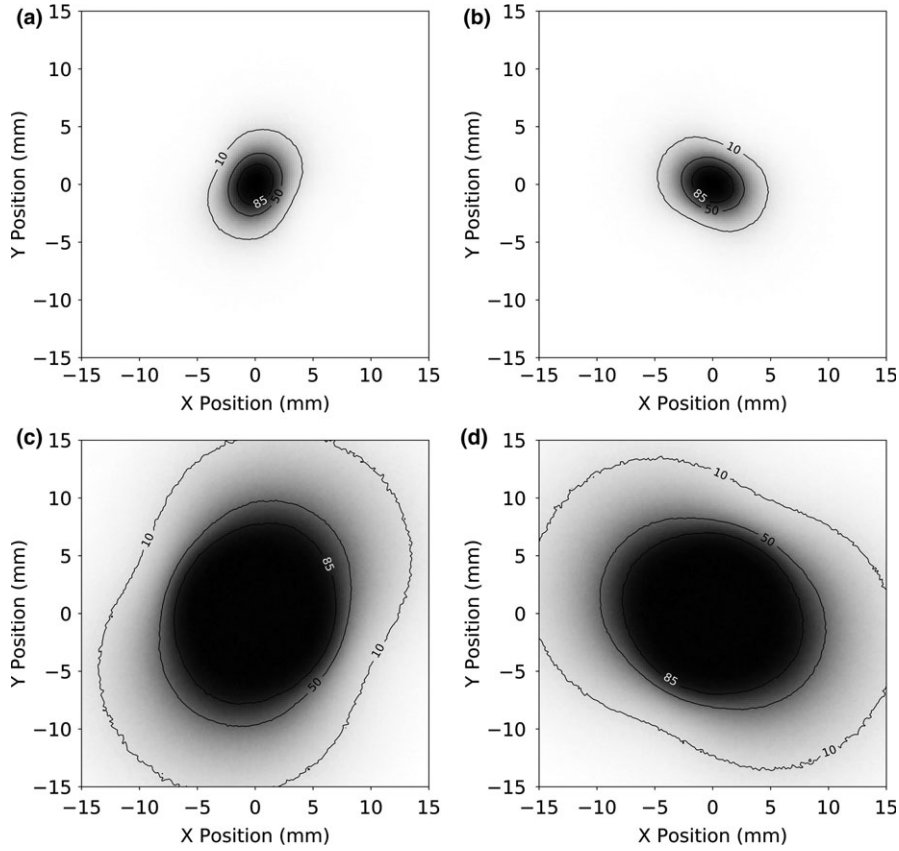

FIG. 7. Simulation of speed modulated radio surgery (SMRS) mode of RGS. (a) and (c) show cosine modulation, while (b) and (d) show sine modulation of the angles for 4 mm and 18 mm sizes of the collimator.

simulated dose distribution for the SMRS mode of the RGS. In Figs. 7(a) and 7(c), the rotational speed of the collimators was a sine function of the angle for the 4 and 18 mm collimators, respectively. For Figs. 7(b) and 7(d), a cosine function was used for the same collimators. The dose distributions produced are similar to the IMRS mode of the RGS. A comparison of the long and short axes of the dose distributions for the 4 and 18 mm collimators are shown in Fig. 8. Figure 8(a) has the comparison of the profiles from the 4 mm collimator configuration, while Fig. 8(b) shows the comparison of profiles from the 18 mm collimator configuration. The dose profile along the short axis has a sharper falloff compared to the dose profile along the long axis. This is similar to the dose profiles obtained from the IMRS mode described in the previous section; however, with a reduced irradiation time. The comparison of the penumbra produced by the IMRS and the SMRS mode are shown in Table II.

The penumbra varies approximately 0.28 mm for the 4 mm collimator configuration, while it varies less than 0.1 mm for the 18 mm collimator configuration.

4. DISCUSSION

Although the normal operation mode of the RGS can safely and effectively treat various lesions, dose spillage into surrounding healthy tissues makes it risky or impossible to treat cases near critical regions at risk. Blocked angle operating of the Gamma Knife® has been shown to effectively treat challenging skull based lesions[22]; however, alternative modalities have not been systematically studied for the RGS. This paper presents the first results of a systematic study of two novel RGS operation modes, IMRS, and SMRS. The normal operation and IMRS modalities were analyzed by comparing the experimental and simulated dose profiles and penumbra. Figure 3 shows that there is a systematic deviation between the simulated and experimental dose profiles, such that the agreement is better for the 4 and 8 mm collimators than for the 14 and 18 mm collimators. Specifically, the simulated falloff and maximum dose regions are in better agreement in the 4 and 8 mm collimators similar to previous model calculations.[8]

In contrast to simulations performed by Cheung et al.,[7] the current simulation shows considerable improvement, as the simulated results agree better with the experimental data as shown in Fig. 4. The percentage differences are more pronounced for the larger collimators; however, all profiles show good agreement. The agreement between the simulated dose profiles and experimental and published data validates the ability of our Geant4-based, Monte Carlo simulations for dose profile and penumbra calculations for the RGS and other SRS devices.

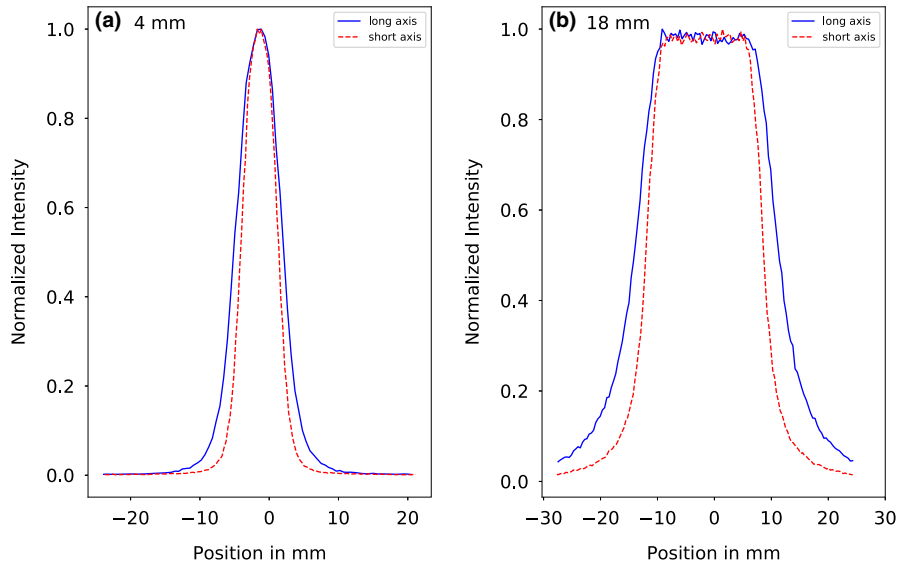

FIG. 8. Profile comparison along the short and long axis for the speed modulated operation in (a) 4 mm and (b) 18 mm configuration. [Color figure can be viewed at wileyonlinelibrary.com]

TABLE II. Comparison of the profile widths between simulations of IMRS and SMRS mode of operation. All penumbra values are calculated as (90% width – 50% width)/2 and are shown are in mm.

		IMRS (mm)			SMRS (mm)		
Collimator size	Axis	90%	50%	Penumbra	90%	50%	Penumbra
4	Long	3.9	7.59	1.85	3.62	7.88	2.13
	Short	2.33	4.9	1.29	2.34	5.2	1.44
18	Long	20.31	27.59	3.64	19.85	27.61	3.87
	Short	16.03	19.33	1.52	15.98	19.21	1.61

The IMRS modality exhibits a sharper dose falloff in the regions where the radiation is blocked. However, the dose delivery time increases in comparison with the normal operation mode. Nonetheless, our results suggest that the RGS IMRS mode could be used to safely target cases near critical regions, such as TN, that it cannot during normal operation.

Results from the SMRS simulations show that this modality produces a sharper penumbra than the normal operation mode in the regions where the orbital speed is increased. However, unlike the IMRS mode where the desired dose accumulates in an intermittent manner, in the SMRS mode the dose accumulates continuously, and thus decreases the time to achieve the desired dose in the center. The speed modulation functions for this study were chosen to allow for comparisons with the IMRS mode; however, we anticipate that more sophisticated functions could further improve critical tissue sparing, as well as target coverage, conformity, and treatment times. In contrast to the spherical shot placement method currently used for the RGS, SMRS may eventually be used to perform a continuous "dose sculpting" procedure for lesions near critical regions, such as the optic nerve and the brainstem, while reducing the overall treatment time.

5. CONCLUSION

The simulated dose profiles and penumbra were found to be in strong agreement with those obtained from measurements for the normal operation mode of the RGS. MC calculations of the dose profiles and penumbra for the IMRS operation mode also show a good agreement with the measurements. When operating in the IMRS mode, the RGS is capable of dose modulation where the dose distribution is highly restrained with sharper penumbra in the regions where the radiation is blocked. Due to the complete blockage of radiation during the procedure, the average dose rate can be factors lower, depending on the size of angular regions blocked. IMRS with the RGS could thus be clinically applicable for the treatment of lesions near vital regions at risk. The SMRS MC calculations reveal that this novel operation mode produces a sharper penumbra in regions where the orbital speed is increased. Unlike the IMRS mode, however, the SMRS mode does not increase the dose delivery time. More sophisticated functions could allow for the continuous delivery of radiation, which would reduce treatment times substantially.

CONFLICT OF INTEREST

The authors have no conflict to disclose.

[a)]Author to whom correspondence should be addressed. Electronic mail: etakacs@g.clemson.edu

REFERENCES

1. Goetsch SJJ, Murphy BDD, Schmidt R, et al. Physics of rotating gamma systems for stereotactic radiosurgery. *Int J Radiat Oncol Biol Phys*. 1999;43:689–696.
2. Wu A, Lindner G, Maitz AH, et al. Physics of gamma knife approach on convergent beams in stereotactic radiosurgery. *Int J Radiat Oncol Biol Phys*. 1990;18:941–949.
3. Lindquist C, Paddick I. The Leksell gamma knife perfexion and comparison with its predecessors. *Oper Neurosurg*. 2007;61(suppl 3):130–141.
4. Régis J, Tamura M, Guillot C, et al. Radiosurgery with the world's first fully robotized Leksell gamma knife perfexion in clinical use. *Neurosurgery*. 2009;64:346–356.
5. Lindquist C, Kihlström L, Hellstrand E. Functional neurosurgery – A future for the gamma knife? *Stereotact Funct Neurosurg*. 1992;57:72–81.
6. Kubo HD, Araki F. Dosimetry and mechanical accuracy of the first rotating gamma system installed in North America. *Med Phys*. 2002;29:2497–2505.
7. Cheung JYC, Yu KN. Rotating and static sources for gamma knife radiosurgery systems: Monte Carlo studies. *Med Phys*. 2006;33:2500–2505.
8. Tian Y, Wang H, Xu Y, et al. Comparison of dosimetric characteristics between stationary and rotational gamma ray stereotactic radiosurgery systems based on Monte Carlo simulation. *Biomed Phys Eng Express*. 2016;2:45014.
9. NINDS. *NINDS: trigeminal neuralgia fact sheet*. https://www.ninds.nih.gov/Disorders/Patient-Caregiver-Education/Fact-Sheets/Trigeminal-Neuralgia-Fact-Sheet. Published 2013. Accessed August 8, 2017.
10. Rogers CLL, Shetter AG, Fiedler JA, Smith KA, Han PP, Speiser BL. Gamma knife radiosurgery for trigeminal neuralgia: the initial experience of the Barrow Neurological Institute. *Int J Radiat Oncol Biol Phys*. 2000;47:1013–1019.
11. Varela-Lema L, Lopez-Garcia M, Maceira-Rozas M, Munoz-Garzon V. Linear accelerator stereotactic radiosurgery for trigeminal neuralgia. *Pain Phys*. 2015;18:15–27.
12. Singh R, Davis J, Sharma S. Stereotactic radiosurgery for trigeminal neuralgia: a retrospective multi-institutional examination of treatment outcomes. *Cureus*. 2016;8:e554.
13. Mammoo D. *Monte Carlo simulation and film dosimetry of rotating gamma system gamma ART-6000 output factors*, 2008. https://search.proquest.com/openview/0ed092111cab3d74faedff1b92363d2c/1?pq-origsite=gscholar&cbl=18750&diss=y
14. Luan S, Swanson N, Chen Z, Ma L. Dynamic gamma knife radiosurgery. *Phys Med Biol*. 2009;54:1579–1591.
15. Allison J, Amako K, Apostolakis J, et al. Geant4 developments and applications. *IEEE Trans Nucl Sci*. 2006;53:270–278.
16. Agostinelli S, Allison J, Amako K, et al. Geant4 – A simulation toolkit. *Nucl Instrum Methods Phys Res A*. 2003;506:250–303.
17. Apostolakis J, Asai M, Bogdanov AG, et al. Geometry and physics of the Geant4 toolkit for high and medium energy applications. *Radiat Phys Chem*. 2009;78:859–873.
18. Allison J, Amako K, Apostolakis J, et al. Recent developments in Geant4. *Nucl Instrum Methods Phys Res A*. 2016;835:186–225.
19. Raman S. A note on 60Co decay. *Zeitschrift für Phys*. 1969;228:387–390.
20. Romano F, Sabini MG, Cuttone G, Russo G, Mongelli V, Foroni R. Geant4-based Monte Carlo simulation of the Leksell Gamma Knife. In: Yu B, ed. *Nuclear Science Symposium Conference Record, Nuclear Science Symposium*. Honolulu, HI, Oct 26–Nov 3, 2007. IEEE; 2007:2581–2586.
21. GEANT4 Collaboration. *Reference physics lists*, 2013. http://geant4.cern.ch/support/proc_mod_catalog/physics_lists/referencePL.shtml. Accessed October 2, 2017.
22. Nakamura JL, Pirzkall A, Carol MP, et al. Comparison of intensity-modulated radiosurgery with gamma knife radiosurgery for challenging skull base lesions. *Int J Radiat Oncol*. 2003;55:99–109.